

Published in final edited form as:

*Sci Transl Med.* 2011 August 31; 3(98): 98ra84. doi:10.1126/scitranslmed.3002152.

## Noninvasive Electroanatomic Mapping of Human Ventricular Arrhythmias Using ECG Imaging (ECGI)

Yong Wang, PhD<sup>1</sup>, Phillip S. Cuculich, MD<sup>1,2</sup>, Junjie Zhang<sup>1</sup>, Kavita A. Desouza, MD<sup>1</sup>, Ramya Vijayakumar<sup>1</sup>, Jane Chen, MD<sup>1,2</sup>, Mitchell N. Faddis, MD, PhD<sup>1,2</sup>, Bruce D. Lindsay, MD<sup>3</sup>, Timothy W. Smith, DPhil, MD<sup>1,2</sup>, and Yoram Rudy, PhD<sup>1,2</sup>

<sup>1</sup>Cardiac Bioelectricity and Arrhythmia Center; Washington University, St. Louis, Missouri

<sup>2</sup>Cardiovascular Diseases, Department of Medicine, Washington University School of Medicine, St. Louis, Missouri

<sup>3</sup>Cardiovascular Medicine, Cleveland Clinic, Cleveland, Ohio

### Abstract

Sudden cardiac death due to ventricular tachycardia (VT) is a major health issue worldwide. Efforts to identify patients at risk, determine VT mechanisms, and effectively prevent and treat VT with a mechanism-based approach would benefit from continuous noninvasive imaging of the arrhythmia over the entire heart. This paper presents the first noninvasive images of human ventricular arrhythmias using electrocardiographic imaging (ECGI), highlighting the large diversity of human VT in terms of activation patterns, mechanisms, and sites of initiation. Based on comparison with catheter mapping, ECGI provided high spatial resolution; a property that overcomes a limitation of the body surface electrocardiogram, which provides only global information. The spatial resolution and ability to image the activation sequences over the entire ventricular surfaces in a single beat allowed us to make observations regarding VT initiation and continuation, and regarding relationships to ventricular substrates, including anatomical scars and abnormal electrophysiological substrate. The ability of ECGI to provide patient-specific physiologic insights, to map the VT activation sequence and to identify the location and depth of VT origin from a single beat has important clinical implications in treating patients with ventricular arrhythmias.

### Introduction

Ventricular arrhythmias of the heart are a major cause of death and disability. In the last several decades implantable and wearable defibrillator technologies have been developed to terminate ventricular tachycardia (VT), a life-threatening regular and repetitive fast heart rhythm, and ventricular fibrillation (VF), an irregular fast heart rhythm that is even more lethal.<sup>1-3</sup> In addition, antiarrhythmic drugs have been developed to prevent VT, with limited success. Invasive procedures to modify the arrhythmic ventricular substrate in order to

**Correspondence:** Yoram Rudy, PhD, FAHA, FHRS, Cardiac Bioelectricity and Arrhythmia Center, Campus Box 1097, One Brookings Drive, Washington University in Saint Louis, Saint Louis, MO 63110, rudy@wustl.edu.

**Note:** First two authors contributed equally to the manuscript.

Author contributions: YW, PSC and YR devised the experiments. YW, PSC, JZ, KAD, RV, JC, MNF, BDL, TWS performed the experiments. YW, PSC, JZ, KAD, RV and YR performed data analysis. YW, PSC, YR wrote the manuscript. All authors reviewed and edited the manuscript. YR provided funding.

Competing interests: Dr. Rudy co-chairs the scientific advisory board of and holds equity in CardioInsight Technologies.

CardioInsight Technologies does not support any research conducted by Dr Rudy, including that presented here. Dr. Lindsay is a member of scientific advisory board of CardioInsight Technologies.

prevent VT have also been used, beginning with cardiac surgery to resect areas of scar.<sup>4-6</sup> More recently, substrate modification has been achieved with radiofrequency ablation delivered at the tip of a steerable catheter, inserted into the heart through a blood vessel.<sup>7-10</sup> Nevertheless, invasive catheter mapping and ablation of the arrhythmic substrate is not a widely available procedure, successful long-term outcomes from the procedure have been modest, and as a result, sudden death from ventricular arrhythmias remains a leading cause of death worldwide. Reasons for this include inability of current diagnostic tools to accurately identify patients at-risk for sudden death, limitations of invasive techniques for intracardiac mapping of cardiac electrical activation during arrhythmia, and incomplete knowledge about how and why VT and VF occur in a particular patient at a particular point in time.

Current noninvasive detection and diagnosis of the cardiac electrical activity is done with a 12-lead electrocardiogram (ECG), a widely used test that is part of routine medical care. However, this century-old technology measures the reflection of cardiac electrical activity on the surface of the body, not on the heart itself. Therefore, it has very limited spatial resolution for determining regional cardiac electrical activity and limited ability to locate regions of arrhythmic activity in the heart. This limitation is especially highlighted when the ECG is compared to currently available cardiac imaging tools, such as echocardiography, computed tomography (CT), and magnetic resonance imaging (MRI). A similar noninvasive imaging method that provides high spatial resolution maps of abnormal electrical activity on the heart surface (rather than on the body surface) could contribute greatly to our understanding of the mechanisms of ventricular arrhythmias and to the diagnosis and treatment of cardiac rhythm disorders in patients. It could also help to identify patients at risk of sudden cardiac death and to develop mechanism-based therapy and guide patient-specific treatments. Here, we present such a noninvasive imaging method (Electrocardiographic Imaging, ECGI) for electroanatomic mapping of cardiac electrical activation, as applied in a series of 25 patients undergoing catheter ablation procedures for various forms of VT.

## Results

ECGI (Figure 1) combines body-surface potentials and heart-torso geometry to noninvasively construct the local electrical signals of the heart (electrograms) over the entire surface of both the left and right ventricles.<sup>11-13</sup> Using the relative timing of the constructed electrograms, activation sequences (isochrones) can be constructed in color-coded maps and the propagation of activation wave fronts can be depicted in animated images (movies). ECGI images are constructed continuously and do not require accumulating data from multiple beats.

Twenty-five patients were referred for evaluation of symptomatic VT or premature ventricular contractions (PVCs). One patient underwent two different studies several months apart, for a total of 26 ECGIs performed. This group of patients underwent a total of 23 catheter-based electrophysiology studies (EPS) with intent to initiate the ventricular arrhythmia, map its origin and circuit (if possible), and ablate the necessary tissue to render the arrhythmia noninducible. Noninvasive ECGI was performed prior to the invasive EPS in those patients who demonstrated spontaneous abnormal ventricular rhythms (18 patients, 19 studies). ECGI was performed during the EPS in other patients (4 patients). Nine patients were imaged during sustained VT; the remainder were imaged during PVCs.

Patients are identified on the basis of their VT localization; RVX for patient X with right ventricular (RV) localization; LVX for patient X with left ventricular (LV) localization. Pertinent medical records are summarized in Table 1. The mean age for the cohort was 54

years (range 21–81 years). Results of the corresponding EPS, including 12-lead ECG morphology, cycle length, and information regarding induction, testing and ablation of the tachycardia are detailed in the Supplemental Material (compiled in supplemental Table S1).

Detailed maps of ventricular arrhythmias for all ECGI studies are available in the Supplemental Material, comprising a collection of noninvasively mapped human VTs. Activation movies are provided for a subset of representative cases. The Supplemental Material also includes a map and movie of a normal ventricular activation pattern, for reference. Representative examples are shown in the text to highlight specific cardiac physiology. ECGI was used to characterize each tachycardia on the basis of analysis of isochrone, potential, local electrogram, and wavefront propagation information. A three-step process, created from previously validated findings<sup>11–13</sup> was used for each patient: (i) localize the site of origin (SOO) of the arrhythmia from isochrone and potential maps; (ii) evaluate the mechanism by observing the three-dimensional propagation pattern and its relation to the myocardial substrate; (iii) approximate the myocardial depth of the origin by using local electrograms (pure Q wave for epicardial origin, rS complex for intramural or endocardial origin).

### LOCATION OF VT INITIATION

On the basis of the invasive EPS, 11 patients had a SOO in the RV, including 9 patients in which the SOO was in the RV outflow tract. Twelve patients had a SOO in the LV. When we compared the results from ECGI to those from invasive EPS (Table 2), ECGI correctly identified the LV or RV SOO 100% of the time (23/23). When we compared the specific locations within each ventricle, noninvasive ECGI SOO was in agreement with invasive EPS SOO in 10/11 RV sites (91%), and 11/12 LV sites (92%). Examples of ECGI localization can be found in Figure 2.

For the two patients with discrepancies between invasive EPS and noninvasive ECGI (patients RV10 and LV11), the discrepant locations were in proximity to each other. For Patient RV10, ECGI imaged the right posterolateral base as the SOO, while EPS suggested the right posteroseptal base as the SOO. This patient had undergone prior ablations of a right posteroseptal accessory pathway and a right atriofascicular pathway in the posterolateral base. We suspect that the prior ablations in these locations may have played a role in the differences between ECGI and EPS. For Patient LV11, ECGI imaged the mid-anterior LV as the SOO, while EPS suggested a more apical LV location as the SOO. This patient had a large LV apical aneurysm, and had several different VT morphologies. It is possible that ECGI and EPS imaged two different VTs.

### MECHANISMS OF VT

During the invasive EPS, the arrhythmia mechanism can be characterized based on the response to ventricular pacing at a faster rate than the tachycardia and resetting of the VT, a process known as entrainment. Based on invasive EPS, 18 patients were found to have focal VT (activation starting from a focal site; inability to reproducibly entrain the tachycardia with ventricular pacing), while 5 had a reentrant mechanism (activation forming a rotational wave comprising nearly all of the tachycardia cycle length; successful entrainment of the tachycardia with stable return cycle lengths after cessation of pacing). For the patients with focal VTs, noninvasive ECGI activation maps uniformly showed a radial activation pattern from the SOO (18/18). In all the patients with a reentrant mechanism, noninvasive ECGI showed a rotational wavefront with a high degree of curvature (5/5), with the wavefront returning to the initiation site. Examples of these two distinct propagation patterns are shown in Figure 3. Detailed descriptions and selected movies of activation are in the Supplemental Material. It should be emphasized that the five reentrant VTs imaged by ECGI

involved a macro-reentry circuit. With its current spatial resolution, ECGI cannot differentiate mechanistically between micro-reentry and focal activation.

The use of ECGI during induction of VT by programmed stimulation in the EP lab allowed us to visualize arrhythmogenesis in a closed-chest human heart. An example is Figure 4, in which programmed ventricular stimulation initiates sustained VT. Figure 4A shows baseline pacing (cycle length = 600ms) from a catheter placed in the RV apex, marked with +. A line of conduction block through which the wavefront cannot directly pass is seen in the lateral LV (thick black line). Figure 4B shows premature pacing ( $S1-S2 = 280\text{ms}$ ) from the same location, resulting in functional extension of the line of block. Figure 4C demonstrates the first beat of induced VT, marked with \*, which originates from the last area that was activated by the premature paced beat in Figure 4B, suggesting triggered activity as the mechanism.<sup>14</sup> The delayed activation of this region by premature pacing promotes recovery and capture of adjacent myocardium by the first beat of VT excitation. In this case, during the invasive EPS, the VT had variable responses to pacing entrainment maneuvers, which is more characteristic of focal triggered activity than reentrant mechanism.

In addition to VT initiation, ECGI provided images of maintenance of VT. As shown in the activation movies LV1 and LV2 in the Supplemental Material, local presystolic activation was often imaged 5–10 ms before the subsequent beats of both reentry and focal VT. The presystolic activation was always near the SOO of the VT and was often consistent from beat to beat. This finding was apparent on ECGI of patients with VT of both epicardial origin (1:02 and 1:13 in Movie LV1) and endocardial origin (0:14, 0:27, and 0:50 in Movie LV2).

For all 5 patients with reentrant VT, the VT activation pattern was related to areas of ventricular scar, as shown in the example of Figure 5. Figure 5B shows ECGI during VT, where the earliest activation is in the inferior basal septum (red). The wavefront initially exits this area at the start of the VT beat and completes the beat by re-entering this area (arrows). Local pre-systolic activation was imaged at the scar border immediately prior to each VT beat, indicating exit sites of slowly propagating wavefronts through the scar (see Movie LV2, Supplemental Material). Figure 5C, left shows results from the clinical nuclear myocardial perfusion images (SPECT). For this study, technetium-99m is administered intravenously and is incorporated into living cardiac myocytes. Imaging the absence of this isotope in regions of the heart allows identification of scar, most often due to a myocardial infarction. In Figure 5C (left), the area of scar from a prior infarction is located in the inferior septum (dark blue). Invasive catheter mapping (Figure 5C, right) during tachycardia confirmed the origin of VT in the inferior septum. Pacing entrainment maneuvers confirmed a reentrant mechanism, and radiofrequency ablation, applied through the tip of a catheter in this region (red marks), terminated the tachycardia.

Although monomorphic VT is thought to arise from a single location, localized beat-to-beat changes in the ventricular activation pattern can be seen with ECGI. This may be a result of different exit points from a ventricular scar (Figure 6), or functional changes related to ventricular excitation and recovery properties, as shown in LV5 in Supplemental Material. Figure 6 shows ECGI during a monomorphic VT from an infiltrative cardiomyopathy in the lateral LV. Figure 6A shows activation patterns for three consecutive VT beats (T1, T2, T3) in three views. ECGI identified two distinct areas of early epicardial activation (white asterisks), which differed slightly from beat to beat. The propagation pattern varies depending on the relative contribution of the two sources, but for all beats the wavefront turns clockwise and propagates toward the LV lateral base with a high degree of curvature, where it reaches a line of block in the inferolateral base. ECGI movies of this phenomenon are available online (Movie LV3). Figure 6B shows a gadolinium-enhanced MRI image,

which revealed a patch of myocardial enhancement in the lateral LV (white arrows), consistent with a focal myocarditis or cardiac sarcoid. Figure 6C shows the invasive electroanatomic map created during the presenting VT (Tx). The region of earliest activation is white (black arrows). Figure 6D shows the invasive electroanatomic map created during a different VT (Ty) after initial ablation at the site of earliest activation. The earliest activation site (black arrows) is shifted more apically. 12-lead surface ECGs of the two VT morphologies (Tx and Ty) are shown. In this example, noninvasive ECGI was able to accurately identify the spontaneous, dynamic beat-to-beat transitions of VT activation patterns, which were not easily recognized on the 12-lead ECG. Examples of similar beat-to-beat changes during VT, imaged by ECGI, can be found in the Supplemental Material (LV5, LV9, LV13).

## MYOCARDIAL DEPTH

Invasive EPS findings were compared with ECGI for determining epicardial or intramural locations of VT. Because of the thin tissue in the outflow tract, patients with outflow tract SOO were excluded. Of the 13 remaining patients, the invasive EPS determined the SOO to be endocardial in 6, epicardial in 5, and midmyocardial in 2. All 5 patients with epicardial SOO had a pure Q wave on the noninvasive ECGI electrogram at the site of earliest activation (100%), indicative of epicardial origin<sup>15</sup>. Of the patients with a nonepicardial SOO, the local noninvasive ECGI electrogram at the earliest site demonstrated a small r wave in 7 of 8 (88%), indicative of an intramural initiation site<sup>15</sup>.

## Discussion

This paper reports the use of a noninvasive, three-dimensional electroanatomic mapping system, ECGI, in a series of patients undergoing catheter ablation for a broad range of VTs. Our findings reveal a large diversity of human VT with respect to activation patterns, mechanisms, and sites of initiation (shown individually, including movies of dynamic progression, in the Supplemental Material). Over a wide range of VT locations and mechanisms, the noninvasive ECGI results were consistent with those of invasive catheter mapping.

In the clinical setting ECGI overcomes the main limitation of the standard body-surface 12-lead ECG by providing high spatial resolution maps of ventricular arrhythmias on the heart surface. Where the 12-lead ECG requires interpretation of body surface data in terms of cardiac activity, assuming a “standard” heart shape and size in a “standard” torso, ECGI uses the patient’s specific heart-torso geometry to identify the location of the arrhythmia and map its sequence on the heart. Additionally, ECGI offers distinct advantages over invasive catheter mapping, including its noninvasive nature and the ability to map the entire tachycardia in a single beat (whereas catheter mapping is done in a “roving probe” approach, collecting data from many beats to complete a map). The spatial resolution and ability to image continuously and simultaneously the activation sequences over the entire ventricular surfaces allowed us to make observations beyond the ability of current tools regarding VT initiation and continuation (Figure 4), and regarding the relationship of the VT activation wavefront to the ventricular substrate (Figures 5, 6), including anatomical scars and abnormal electrophysiological substrate (lines of block, slow conduction). With the single beat, continuous mapping that ECGI provides, we were able to detect beat – to – beat dynamic changes in the origin and sequence of VT (Figure 6).

The results suggest a clinically useful role for ECGI. From a treatment perspective, potential clinical advantages include the ability to assist in guiding the choice of medication on the basis of VT mechanism, or pointing to the most effective strategy for catheter ablation. An example could illustrate the potential benefit. Currently, when a patient has recurrent VT,

especially when it is refractory to antiarrhythmic medications, an EP study with ablation is offered. An endocardial approach (through veins) is almost exclusively used as a first procedure, and the operator tries to induce the arrhythmia. The VT can only be mapped accurately if it is both sustained and hemodynamically tolerated, which is the case less than half the time. Mapping is a meticulous process, collecting electrical information from the tip of a roving catheter on a point-by-point basis, lasting several hours. Ideally, for obtaining a detailed map of the arrhythmia, the mapping is performed during sustained VT. However, this can have deleterious cardiovascular effects. If at the end of mapping, or after unsuccessful endocardial ablation, the operator deems the VT to be epicardial in origin, the procedure is halted and a separate procedure to target the epicardium is scheduled at a later date. In contrast, if ECGI is used, the location and depth of the VT can be determined in a single beat of arrhythmia, either during or before the procedure. The treating physician could then direct the procedure toward that area, in a more focused and time-efficient manner, with the goal of improved patient safety and beneficial treatment outcomes. This potential application requires evaluation in a randomized clinical trial in a large population of VT patients.

Looking to the future, the ability to diagnose and treat arrhythmias in an entirely noninvasive way would be a major advancement. The results presented here provide the basis for noninvasive arrhythmia diagnosis, while technologies such as high-frequency ultrasound<sup>16,17</sup> and gamma-knife radiosurgery<sup>18</sup> are being developed for noninvasive ablation of cardiac tissue. The noninvasive nature of the approach would also make it possible to conduct follow-up ECGI tests to evaluate outcomes of treatment (by ablation or drugs) and examine changes over time.

There are several limitations to the clinical applicability of ECGI at this time. ECGI is still a novel research tool and its limited availability precludes large-scale multicenter clinical studies at present. Further technical developments are needed to facilitate fast application of the many body surface electrodes in the clinical setting, automate the data analysis and map generation and display, and build a user friendly interface for the clinical operator. The body surface electrodes, placed with high density on the torso surface, often compete for skin area needed to place other clinical monitoring systems during the EP study. Finally, previous ECGI validation studies show accuracy of 4–6 mm in determining activation initiation sites. Future algorithm developments may allow for more precise mapping.

The most significant weakness to the current study involves the variable contributions of the endocardium and epicardium to tachycardia circuits<sup>19–22</sup>. As demonstrated in open chest mapping, the earliest epicardial activation of VT may not accurately identify the location of an endocardial circuit, although our data show close correlation between invasive endocardial mapping and noninvasive ECGI epicardial imaging. Additionally, because the ECGI-imaged activation sequence only uses the QRS complex for analysis, it does not image the entire time during one cycle of tachycardia, known as cycle length. Slow, discontinuous diastolic conduction inside the scar (reflected in early activation detected by ECGI at the scar borderzone; see example in Movie LV2) and intramural activation (ECGI is limited to the epicardium) likely continue during the time that ECGI does not image. Finally, analysis of the ECGI data collected in the EP lab (4 out of the 26 cases) was subject to bias of knowing the outcome of the EPS.

## Materials and Methods

All protocols were approved by the Institutional Review Board at Washington University in St. Louis, and informed consent was obtained from all patients. ECGI methodology was described previously.<sup>11–13</sup> ECGI has been validated extensively under different

physiological and pathological conditions in animal models<sup>13,15,23–26</sup> and in human studies<sup>11,12,27–42</sup>. 256 carbon electrodes on strips were applied to the patient's torso. Small radioopaque markers were attached to each electrode. All strips were connected to a portable mapping system (BioSemi). After electrodes application, patients underwent thoracic non-contrast gated computed tomography (CT) scan with axial resolution of 3mm. Scans were gated at 70% of the R-R interval (ventricular diastole) if patients were in sinus rhythm. For patients who underwent continued ECGI mapping during a subsequent EP study, the 256 carbon electrodes were kept in the same position. Patientspecific ventricular epicardial surface geometry and body surface electrode positions were labeled and digitized from CT images.

The 256 channels of body surface potentials were sampled at 1-ms intervals, and the data were saved on a laptop computer. Body surface potentials were acquired during sinus rhythm, VT, and programmed electrical stimulation, when available.

The body surface potential and geometrical information (torso-heart geometrical relationship) were combined by ECGI algorithms to noninvasively construct epicardial electrograms, activation sequences (isochrones), potential maps, and repolarization patterns.<sup>11,12</sup> ECGI was constructed on a beat-by-beat basis and did not require accumulating data from many identical beats. Activation times were determined by the maximal negative slope of the epicardial electrograms. Activation movies for several consecutive beats were constructed by animating the activation wave front on the patient-specific CT-derived epicardial surface. On the basis of the isochrone map, lines or regions of block (thick black lines in the map) were inferred if activation times in adjacent areas differed by more than 50ms. Slow conduction is represented by crowded isochrones. The earliest site of epicardial activation was determined from the isochrones map and from the earliest potential minimum in the epicardial potential map.<sup>13</sup>

The results of ECGI were processed independently from the results of the EP study. Additionally, EP operators did not have access to ECGI results prior to the procedure. Clinical cardiac testing results, such as invasive three-dimensional electroanatomic maps, gadolinium-enhanced cardiac magnetic resonance imaging (MRI) and single-photon emission computed tomography (SPECT), were obtained retrospectively for each patient.

## Supplementary Material

Refer to Web version on PubMed Central for supplementary material.

## Acknowledgments

We thank Tim Street and Subham Ghosh for their help in this study. Yoram Rudy is the Fred Saigh Distinguished Professor at Washington University in St Louis.

Funding: This study was supported by NIH-NHLBI grants R01-HL-033343-26 and R01HL- 049054-18 (to Yoram Rudy) and Grants 1 UL1 RR024992-01, 1 TL1 RR024995-01 and 1 KL2 RR 024994-01 from the National Center for Research Resources (NCRR) of the NIH.

## References

1. Moss AJ, Hall WJ, Cannom DS, Daubert JP, Higgins SL, Klein H, Levine JH, Saksena S, Waldo AL, Wilber D. Improved survival with an implanted defibrillator in patients with coronary disease at high risk for ventricular arrhythmia. Multicenter Automatic Defibrillator Implantation Trial Investigators. *N. Engl. J. Med.* 1996; 335:1933–1940. [PubMed: 8960472]

2. A comparison of antiarrhythmic-drug therapy with implantable defibrillators in patients resuscitated from near-fatal ventricular arrhythmias. The Antiarrhythmics versus Implantable Defibrillators (AVID) Investigators. *N. Engl. J. Med.* 1997; 337:1576–1583. [PubMed: 9411221]
3. Buxton AE, Lee KL, Fisher JD, Josephson ME, Prystowsky EN, Hafley G. A randomized study of the prevention of sudden death in patients with coronary artery disease. Multicenter Unsustained Tachycardia Trial Investigators. *N. Engl. J. Med.* 1999; 341:1882–1890. [PubMed: 10601507]
4. Wittig JH, Boineau JP. Surgical treatment of ventricular arrhythmia using epicardial, transmural, and endocardial mapping. *Ann Thorac Surg.* 1975; 20:117–126.
5. Guiraudon G, Fontaine G, Frank R, Escande G, Etievent P, Cabrol C. Encircling endocardial ventriculotomy: a new surgical treatment for life-threatening ventricular tachycardias resistant to medical treatment following myocardial infarction. *Ann Thorac Surg.* 1978; 26:438–444. [PubMed: 753158]
6. Horowitz LN, Harken AH, Kastor JA, Josephson ME. Ventricular resection guided by epicardial and endocardial mapping for treatment of recurrent ventricular tachycardia. *N Engl J Med.* 1980; 302:589–593. [PubMed: 7351905]
7. Marchlinski FE, Callans DJ, Gottlieb CD, Zado E. Linear ablation lesions for control of unmappable ventricular tachycardia in patients with ischemic and nonischemic cardiomyopathy. *Circulation.* 2000; 101:1288–1296. [PubMed: 10725289]
8. Arenal A, Glez-Torrecilla E, Ortiz M, Villacastin J, Fdez-Portales J, Sousa E, del Castillo S, Perez de Isla L, Jimenez J, Almendral J. Ablation of electrograms with an isolated, delayed component as treatment of unmappable monomorphic ventricular tachycardias in patients with structural heart disease. *J. Am. Coll. Cardiol.* 2003; 41:81–92. [PubMed: 12570949]
9. Stevenson WG. Catheter ablation of monomorphic ventricular tachycardia. *Curr. Opin. Cardiol.* 2005; 20:42–47. [PubMed: 15596959]
10. Reddy VY, Reynolds MR, Neuzil P, Richardson AW, Tabonsky M, Jongnarangin K, Kralovec S, Sediva L, Ruskin JN, Josephson ME. Prophylactic catheter ablation for the prevention of defibrillator therapy. *N. Engl. J. Med.* 2007; 357:2657–2665. [PubMed: 18160685]
11. Ramanathan C, Ghanem RN, Jia P, Ryu K, Rudy Y. Noninvasive electrocardiographic imaging for cardiac electrophysiology and arrhythmia. *Nat. Med.* 2004; 10:422–428. [PubMed: 15034569]
12. Ramanathan C, Jia P, Ghanem R, Ryu K, Rudy Y. Activation and repolarization of the normal human heart under complete physiological conditions. *Proc. Natl.Acad. Sci. U. S. A.* 2006; 103:6309–6314. [PubMed: 16606830]
13. Oster HS, Taccardi B, Lux RL, Ershler PR, Rudy Y. Noninvasive electrocardiographic imaging: reconstruction of epicardial potentials, electrograms, and isochrones and localization of single and multiple electrocardiac events. *Circulation.* 1997; 96:1012–1024. [PubMed: 9264513]
14. Moak JP, Rosen MR. Induction and termination of triggered activity by pacing in isolated canine Purkinje fibers. *Circulation.* 1984; 69:149–162. [PubMed: 6689639]
15. Oster HS, Taccardi B, Lux RL, Ershler PR, Rudy Y. Electrocardiographic imaging: noninvasive characterization of intramural myocardial activation from inverse-reconstructed epicardial potentials and electrograms. *Circulation.* 1998; 97:1496–1507. [PubMed: 9576431]
16. Zimmer J, Hynynen K, He D, Marcus F. The feasibility of using ultrasound for cardiac ablation. *IEEE Trans Biomed Eng.* 1995; 42:891–897. [PubMed: 7558063]
17. Strickberger SA, Tokaro T, Kluiwstra J-UA, Morady F, Cain C. Extracardiac Ablation of the Canine Atrioventricular Junction by Use of High-Intensity Focused Ultrasound. *Circulation.* 1999; 100:203–208. [PubMed: 10402451]
18. Sharma A, Wong D, Weidlich G, Fogarty T, Jack A, Sumanaweera T, Maguire P. Noninvasive stereotactic radiosurgery (CyberHeart) for creation of ablation lesions in the atrium. *Heart Rhythm.* 2010; 7:802–810. [PubMed: 20156591]
19. Kaltenbrunner W, Cardinal R, Dubuc M, Shenasa M, Nadeau R, Tremblay G, Vermeulen M, Savard P, Page PL. Epicardial and endocardial mapping of ventricular tachycardia in patients with myocardial infarction. Is the origin of the tachycardia always subendocardially localized? *Circulation.* 1991; 84:1058–1071. [PubMed: 1884439]



20. Harris L, Downar E, Mickleborough L, Shaikh N, Parson I. Activation sequence of ventricular tachycardia: endocardial and epicardial mapping studies in the human ventricle. *J. Am. Coll. Cardiol.* 1987; 10:1040–1047. [PubMed: 3499455]
21. Littmann L, Svenson RH, Gallagher JJ, Selle JG, Zimmern SH, Fedor JM, Colavita PG. Functional role of the epicardium in postinfarction ventricular tachycardia. Observations derived from computerized epicardial activation mapping, entrainment and epicardial laser photoablation. *Circulation.* 1991; 83:1577–1591. [PubMed: 2022017]
22. de Bakker JMT JMT, Janse MJ, van Cappelle FJL, Durrer D. Endocardial mapping by simultaneous recording of endocardial electrograms during cardiac surgery for ventricular aneurysm. *J. Am. Coll. Cardiol.* 1983; 2:947–953. [PubMed: 6630770]
23. Burnes JE, Taccardi B, Rudy Y. A noninvasive imaging modality for cardiac arrhythmias. *Circulation.* 2000; 102:2152–2158. [PubMed: 11044435]
24. Burnes JE, Taccardi B, MacLeod RS, Rudy Y. Noninvasive ECG imaging of electrophysiologically abnormal substrates in infarcted hearts: a model study. *Circulation.* 2000; 101:533–540. [PubMed: 10662751]
25. Burnes JE, Taccardi B, Ershler PR, Rudy Y. Noninvasive electrocardiographic imaging of substrate and intramural ventricular tachycardia in infarcted hearts. *J. Am. Coll. Cardiol.* 2001; 38:2071–2078. [PubMed: 11738317]
26. Ghanem RN, Burnes JE, Waldo AL, Rudy Y. Imaging dispersion of myocardial repolarization, II: noninvasive reconstruction of epicardial measures. *Circulation.* 2001; 104:1306–1312. [PubMed: 11551884]
27. Ghanem RN, Jia P, Ramanathan C, Ryu K, Markowitz A, Rudy Y. Noninvasive electrocardiographic imaging (ECGI): comparison to intraoperative mapping in patients. *Heart Rhythm.* 2005; 2:339–354. [PubMed: 15851333]
28. Intini A, Goldstein RN, Jia P, Ramanathan C, Ryu K, Giannattasio B, Gilkeson R, Stambler BS, Brugada P, Stevensn WG, Rudy Y. Electrocardiographic imaging (ECGI), a novel diagnostic modality used for mapping of focal left ventricular tachycardia in a young athlete. *Heart Rhythm.* 2005; 2:1250–1252. [PubMed: 16253916]
29. Jia P, Ramanathan C, Ghanem RN, Ryu K, Varma N, Rudy Y. Electrocardiographic imaging of cardiac resynchronization therapy in heart failure: observation of variable electrophysiologic responses. *Heart Rhythm.* 2006; 3:296–310. [PubMed: 16500302]
30. Wang Y, Cuculich PS, Woodard PK, Lindsay BD, Rudy Y. Focal atrial tachycardia after pulmonary vein isolation: noninvasive mapping with electrocardiographic imaging (ECGI). *Heart Rhythm.* 2007; 4:1081–1084. [PubMed: 17675084]
31. Wang Y, Schuessler RB, Damiano RJ, Woodard PK, Rudy Y. Noninvasive electrocardiographic imaging (ECGI) of scar-related atypical atrial flutter. *Heart Rhythm.* 2007; 4:1565–1567. [PubMed: 17996498]
32. Wang Y, Li L, Cuculich PS, Rudy Y. Electrocardiographic imaging of ventricular bigeminy in a human subject. *Circ. Arrhythm. Electrophysio.* 2008; 1:74–75.
33. Ghosh S, Rhee EK, Avari JN, Woodard PK, Rudy Y. Cardiac memory in patients with Wolff-Parkinson-White syndrome: noninvasive imaging of activation and repolarization before and after catheter ablation. *Circulation.* 2008; 118:907–915. [PubMed: 18697818]
34. Ghosh S, Avari JN, Rhee EK, Woodard PK, Rudy Y. Noninvasive electrocardiographic imaging (ECGI) of epicardial activation before and after catheter ablation of the accessory pathway in a patient with Ebstein anomaly. *Heart Rhythm.* 2008; 5:857–860. [PubMed: 18482872]
35. Ghosh S, Avari JN, Rhee EK, Woodard PK, Rudy Y. Hypertrophic cardiomyopathy with preexcitation: insights from noninvasive electrocardiographic imaging (ECGI) and catheter mapping. *J. Cardiovasc. Electrophysiol.* 2008; 19:1215–1217. [PubMed: 18479334]
36. Ghosh S, Avari JN, Rhee EK, Woodard PK, Rudy Y. Noninvasive electrocardiographic imaging (ECGI) of a univentricular heart with Wolff-Parkinson-White syndrome. *Heart Rhythm.* 2008; 5:605–608. [PubMed: 18325851]
37. Wang Y, Rudy Y. Electrocardiographic imaging of normal human atrial repolarization. *Heart Rhythm.* 2009; 6:582–583. [PubMed: 19138573]

38. Silva JN, Ghosh S, Bowman TM, Rhee EK, Woodard PK, Rudy Y. Cardiac resynchronization therapy in pediatric congenital heart disease: insights from noninvasive electrocardiographic imaging. *Heart Rhythm*. 2009; 6:1178–1185. [PubMed: 19632630]
39. Varma N, Jia P, Ramanathan C, Rudy Y. RV electrical activation in heart failure during right, left, and biventricular pacing. *JACC Cardiovasc. Imaging*. 2010; 3:567–575. [PubMed: 20541711]
40. Cuculich PS, Wang Y, Lindsay BD, Vijayakumar R, Rudy Y. Noninvasive real-time mapping of an incomplete pulmonary vein isolation using electrocardiographic imaging (ECGI). *Heart Rhythm*. 2010; 7:1316–1317. [PubMed: 20097620]
41. Cuculich PS, Wang Y, Lindsay BD, Faddis MN, Schuessler RB, Damiano RJ, Li L, Rudy Y. Noninvasive characterization of epicardial activation in humans with diverse atrial fibrillation patterns. *Circulation*. 2010; 122:1364–1372. [PubMed: 20855661]
42. Ghosh S, Cooper DH, Vijayakumar R, Zhang J, Pollack S, Haissaguerre M, Rudy Y. Early repolarization associated with sudden death: insights from noninvasive electrocardiographic imaging. *Heart Rhythm*. 2010; 7:534–537. [PubMed: 20153422]
43. Ouyang F, Fotuhi P, Ho SY, Hebe J, Volkmer M, Goya M, Burns M, Antz M, Ernst S, Cappato R, Kuck KH. Repetitive monomorphic ventricular tachycardia originating from the aortic sinus cusp: electrocardiographic characterization for guiding catheter ablation. *J Am Coll Cardiol*. 2002; 39:500–508. [PubMed: 11823089]
44. Lin D, Ilkhanoff L, Gerstenfeld E, Dixit S, Beldner S, Bala R, Garcia F, Callans D, Marchlinski FE. Twelve-lead electrocardiographic characteristics of the aortic cusp region guided by intracardiac echocardiography and electroanatomic mapping. *Heart Rhythm*. 2008; 5 663-339.

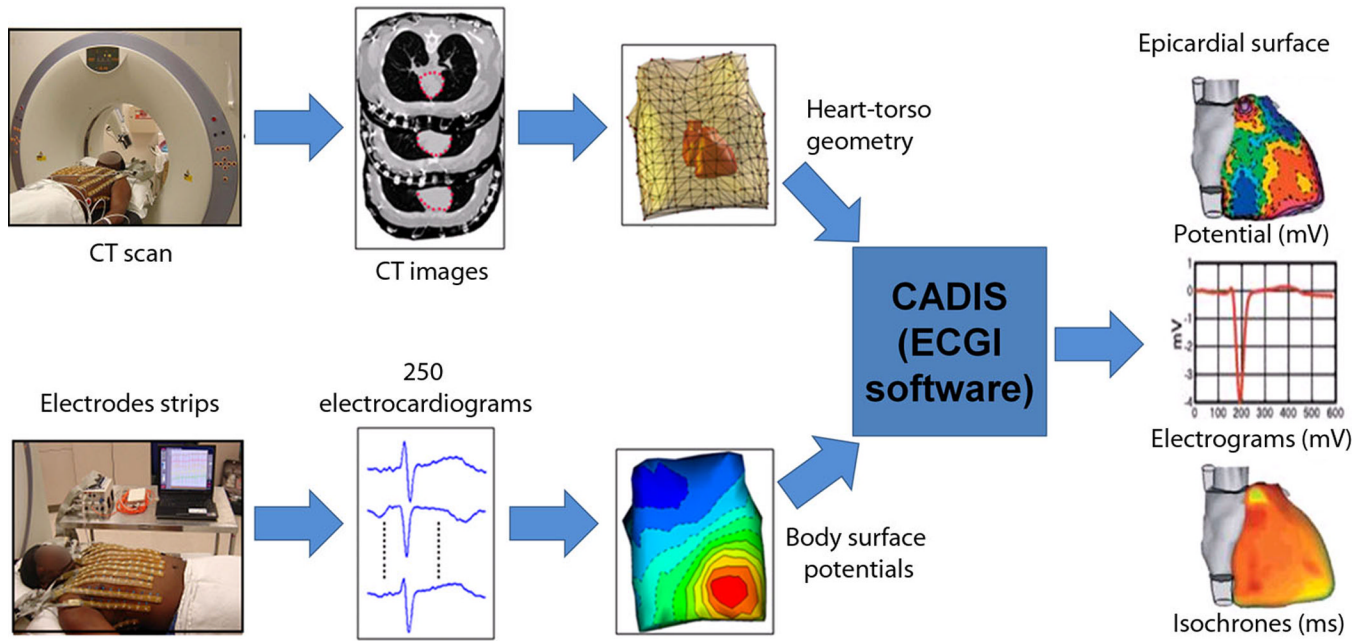


**Figure 1. ECGI methodology**

250 carbon electrodes mounted in strips are applied to the patient's torso before a pre-procedural thoracic CT scan, which provides cardiac geometry and torso-electrode positions in the same reference frame. The electrodes are connected to a multi-channel mapping system. The electrical and anatomical data are processed mathematically to obtain noninvasive ECGI epicardial images that include potential maps, electrograms, isochronal activation sequences, and repolarization patterns. An ECGI movie of normal epicardial activation is provided in the Supplemental Material as reference (control) for the VT data (MOVIE N1).

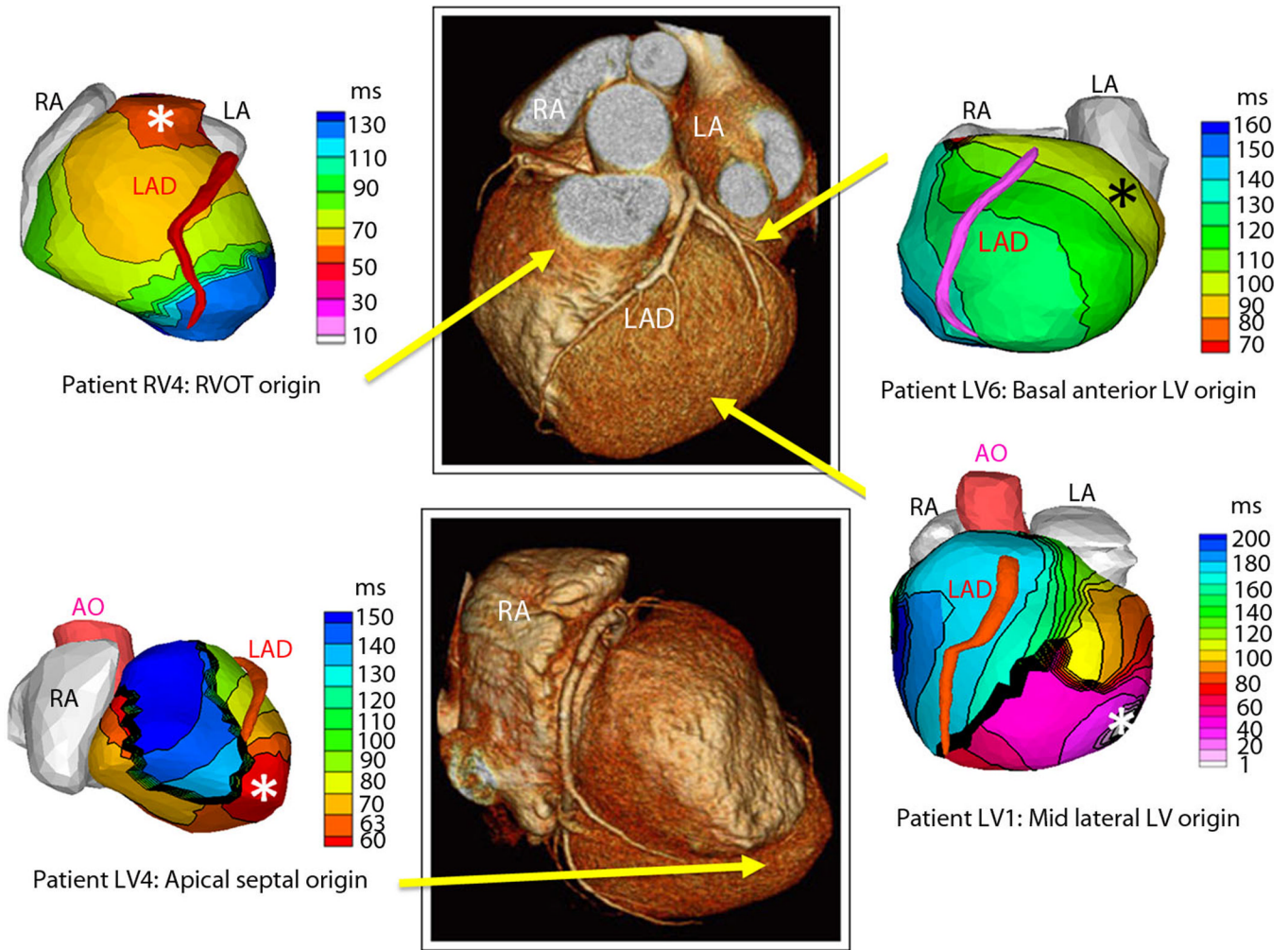
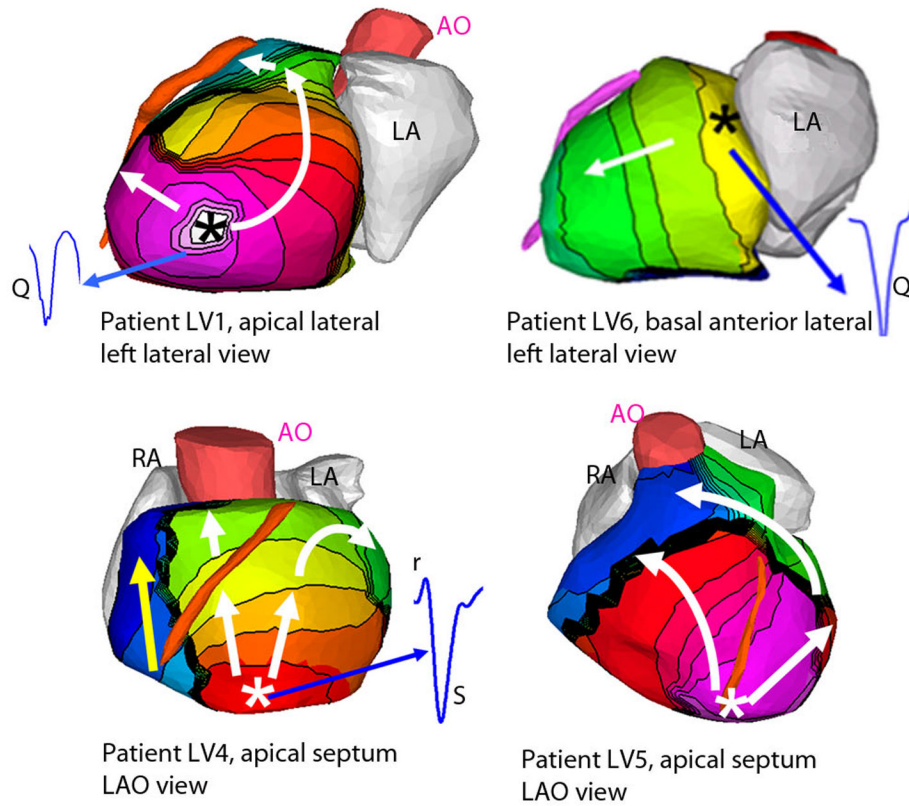


**Figure 2. Examples of noninvasive ECGI isochrone maps for localization of VT site of origin**  
 Epicardial isochrone maps are shown for four patients, with earliest epicardial activation marked with an asterisk (see Supplemental Material for detailed description of activation sequences). EP-study-determined sites of origin are indicated under the ECGI maps. Yellow arrows point to VT origin on a representative CT scan. RA: right atrium; LA: left atrium; AO: aorta; LAD: left anterior descending coronary artery; LV: left ventricle; RVOT: right ventricular outflow tract.

### Focal propagation patterns



### Reentrant propagation patterns

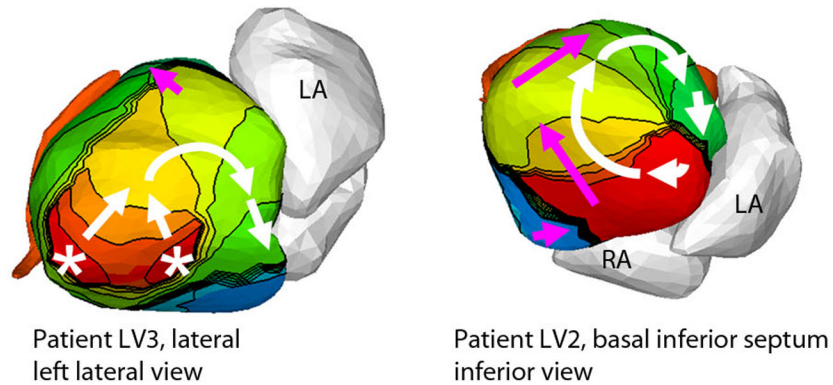


**Figure 3. ECGI imaged propagation patterns, origins, and local electrograms for VT**  
 Isochrone maps are shown for six patients, with earliest epicardial activation marked with an asterisk (see Supplemental Material for detailed descriptions of activation sequences). (Top): Tachycardias that were determined to be focal during EP studies demonstrate a radial spread (white arrows) away from the early activation point (asterisk). Yellow arrows indicate later phases of ventricular activation. (Bottom): Tachycardias that were determined to be reentrant during EP studies show a rotational activation pattern (white arrows). Thick black lines indicate conduction block. Pink arrows indicate later phases of ventricular activation. (Insets): Several epicardial electrograms from sites of earliest activation are shown in blue, highlighting the presence or absence of r-wave; pure Q morphology indicates epicardial

origin, rS morphology indicates intramural origin. Legend under each image indicates the location of VT initiation and identifies the displayed view of the heart; LAO = left anterior oblique.

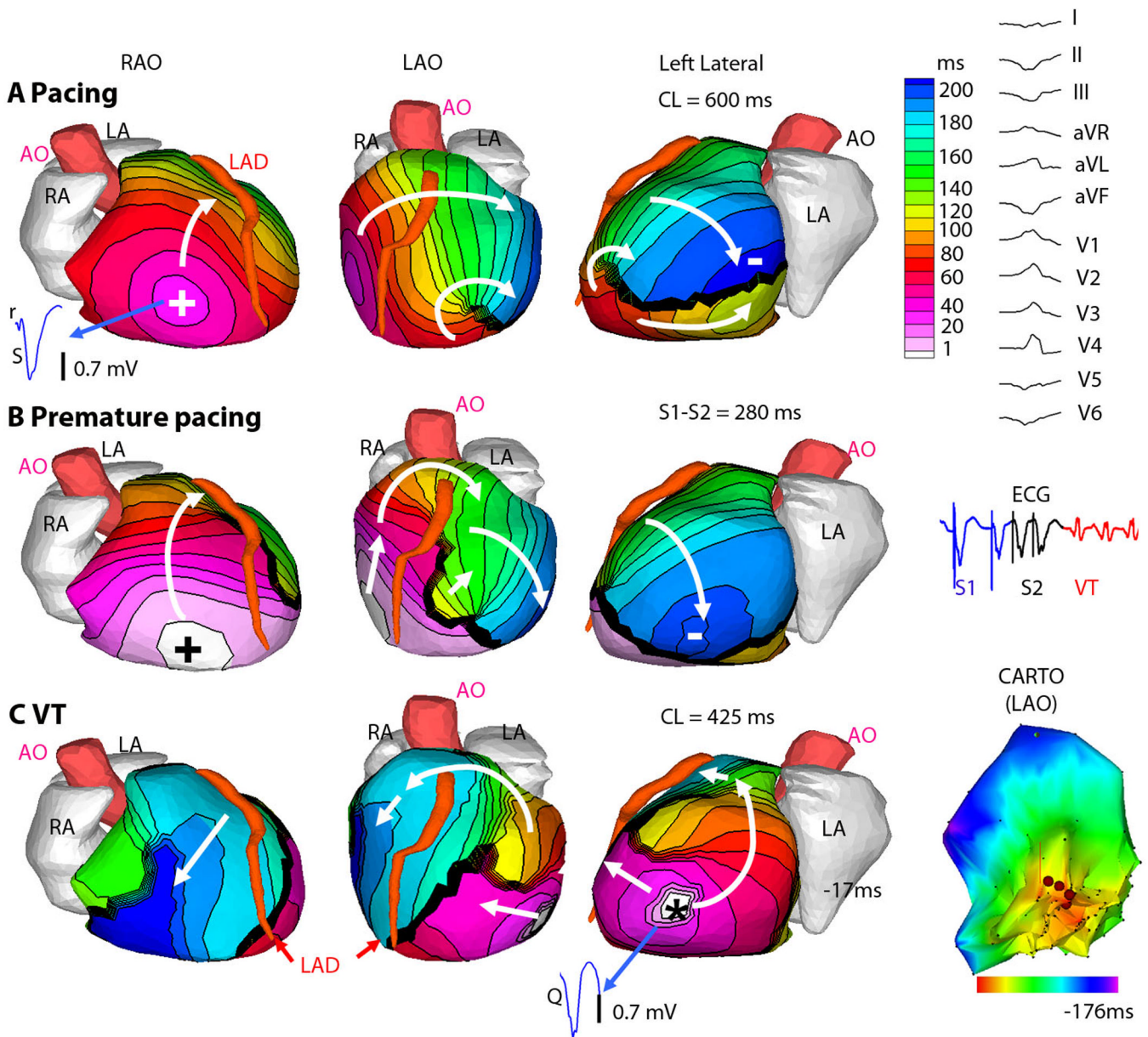


**Figure 4. ECGI of focal VT induced by programmed electrical stimulation (patient LV1)**  
 (A) Epicardial activation sequence during drive train (S1) pacing at cycle length of 600ms. (RAO, right anterior oblique, LAO, left anterior oblique). White arrows show direction of wavefront propagation. Thick black line indicates conduction block. Earliest epicardial activation site is marked by + and corresponds to the underlying endocardial pacing site. ECGI epicardial electrogram from this site is shown (blue), with rS complex consistent with endocardial activation. (Right) The 12-lead surface ECG during VT. (B) Premature (S2) pacing at 280ms coupling interval from the same pacing site. The major wave front is forced to pivot around the extended line of block. There is some fusion with an intramural transeptal front (small white arrow). (Right) A single lead ECG is shown. All S1 beats (blue) are similar, as are the two S2 beats (black) and all VT beats (red) (C) VT; earliest epicardial activation site is marked by asterisk. ECGI electrogram from the VT origin site is shown (blue), with a pure Q wave, indicative of epicardial origin. (Right) Invasive LV

endocardial activation map (CARTO) of the VT in LAO projection, (red is early). ECGI epicardial activation movies are in the Supplemental Material (Movie LV1).



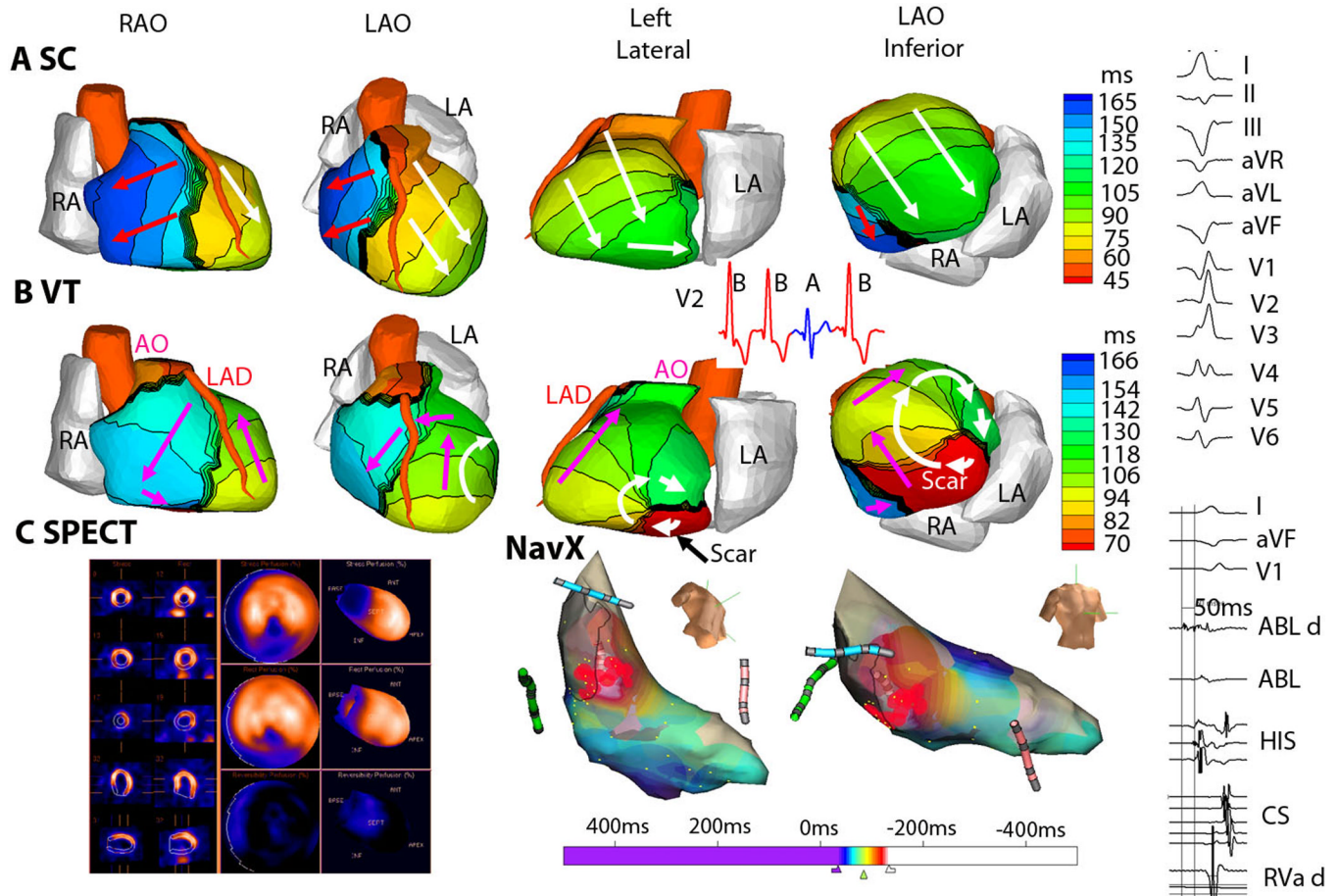


**Figure 5. ECGI of reentrant VT from inferobasal scar (patient LV2)**

(A) Four views of activation sequence during a sinus capture (SC) beat (labeled A, blue on the V2 ECG). Arrows indicate direction of the activation wavefronts. (B) Activation sequence during VT beats (labeled B, red on the V2 ECG). White arrows indicate a clockwise lateral loop (left lateral and LAO inferior views); Pink arrows show propagation into the RV in a counter-clockwise fashion. (C) (Left) SPECT images showing a scar at the inferobasal LV region (blue). (Right) Limited invasive endocardial map of VT activation (red early, blue late). ECGI epicardial activation movies, including early activation of a region near the inferior scar border, are in Supplemental Material (Movie LV2). (Right Column) The 12-lead surface ECG during VT and the ablation-catheter signals. The earliest electrogram signal is seen at the inferoseptal borderzone, 50 ms before onset of the surface QRS.

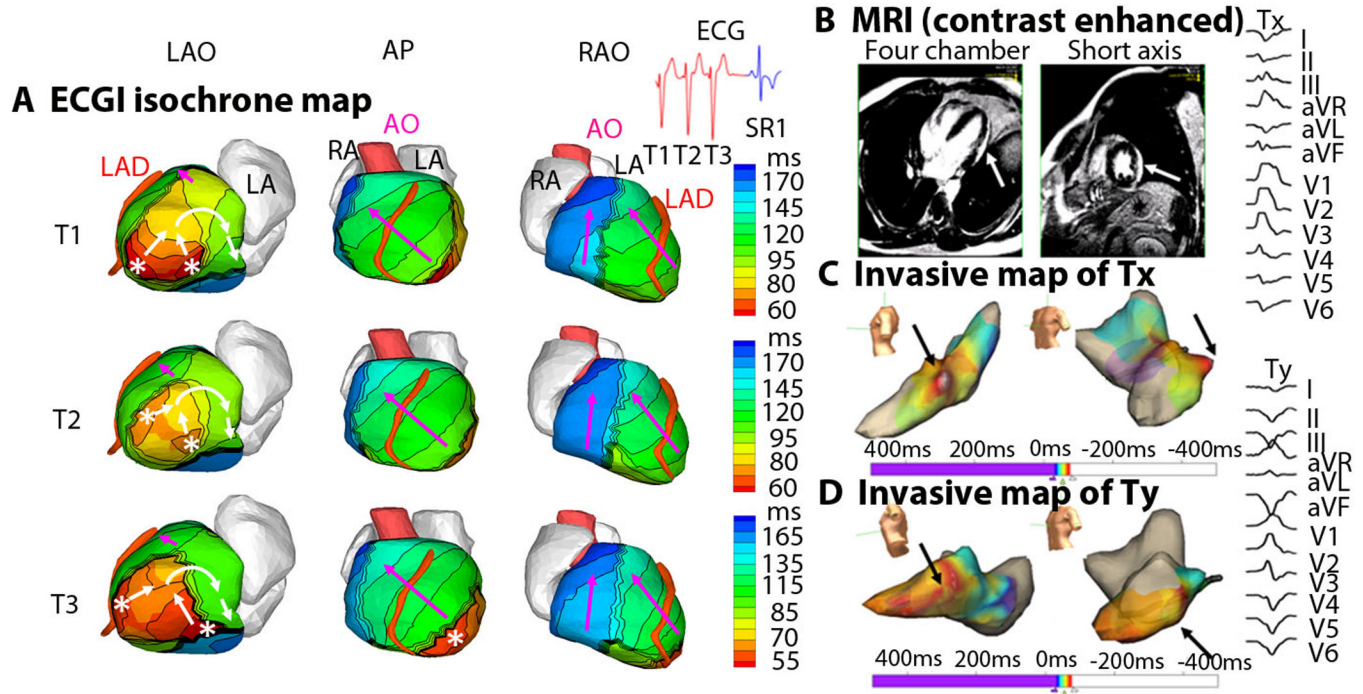


**Figure 6. ECGI of reentrant VT in lateral wall infiltrative cardiomyopathy (patient LV3)**  
 (A) Activation patterns for three consecutive VT beats (T1, T2, T3). ECGI identified two distinct areas of early epicardial activation (white asterisks), which differed from beat to beat. The propagation pattern varied somewhat based on the relative contribution of the two sources, but for all beats the wavefront turns clockwise and propagates to the LV lateral base with a high degree of curvature, where it reaches a line of block in the inferolateral base. ECGI epicardial activation movie is available in the Supplemental Material. (B) A gadolinium-enhanced MRI revealed a patch of myocardial enhancement in the lateral LV (white arrows), consistent with a focal myocarditis or cardiac sarcoid. (C) The invasive electroanatomic map created during the presenting VT (arbitrarily named Tx). The region of earliest activation is white (black arrows). (D) The invasive electroanatomic map created during a different VT (arbitrarily named Ty) after the initial ablation at the site of earliest activation. The earliest activation (black arrows) is shifted more apically. (Right) 12-lead surface ECGs of two VT morphologies (Tx and Ty). AP = anterior-posterior view; SR1 = first sinus rhythm beat after VT.

Table 1

**Patient Population**

Patients are identified on the basis of VT localization; RVX for patient X with right ventricular localization; LVX for patient X with left ventricular localization. PVC: premature ventricular complex; VT: ventricular tachycardia

Patient number	Age, Gender	Clinical Presentation	Ejection Fraction	Ventricular Substrate	Antiarrhythmic Medication
RV1	40, Female	Sustained VT	60%	Inferior nonischemic scar	β-blocker
RV2	42, Male	Nonsustained VT	70%	No scar	β-blocker
RV3	57, Female	Sustained VT	65%	No scar	β-blocker
RV4	21, Male	Nonsustained VT	58%	No scar	β-blocker
RV5	75, Male	Sustained VT	35%	Anterior ischemic scar	β-blocker
RV6	51, Female	Sustained VT	55%	No scar	Amiodarone, β-blocker
RV7	46, Female	Nonsustained VT	60%	No scar	β-blocker
RV8	37, Female	Syncope, Nonsustained VT	55%	No scar	Sotalol, β-blocker
RV9	57, Male	High burden PVCs	40%	Nonischemic cardiomyopathy	Sotalol, β-blocker
RV10	52, Female	Symptomatic PVCs	50%	Minimal scar, with prior ablation	β-blocker
RV11	53, Male	Symptomatic PVCs	60%	No scar	None
LV1	63, Female	Sustained VT	10%	Nonischemic cardiomyopathy	Amiodarone, mexiletine, β-blocker
LV2	58, Male	Sustained VT	40%	Inferior ischemic scar	β-blocker
LV3	45, Male	Syncope, sustained VT	55%	Lateral nonischemic scar (sarcoïd)	β-blocker, lidocaine
LV4	35, Male	Sustained VT	70%	No scar	Calcium channel blocker
LV5	52, Female	Sustained VT	65%	No scar	Amiodarone
LV6	46, Male	Sustained VT	40%	Anterolateral nonischemic scar (sarcoïd)	Sotalol, mexiletine, β-blocker
LV7	48, Female	Nonsustained VT	40%	Nonischemic cardiomyopathy	β-blocker
LV8	71, Male	Sustained VT	40%	Valvular cardiomyopathy	Sotalol
LV9	71, Male	Sustained VT	25%	Inferior ischemic scar	Amiodarone, lidocaine
LV10	42, Male	Syncope, PVCs	45%	Nonischemic (Kawasaki Disease)	β-blocker
LV11	71, Male	Sustained VT	25%	Anterior ischemic scar	Amiodarone
LV12	81, Male	Syncope, sustained VT	30%	Anterior, inferior and lateral ischemic scar	Amiodarone, β-blocker
LV13	62, Male	Sustained VT	30%	Nonischemic cardiomyopathy	Amiodarone, mexiletine, β-blocker
LV14	67, Male	Sustained VT	25%	Apical ischemic scar	Amiodarone, mexiletine, β-blocker

Patient number	Age, Gender	Clinical Presentation	Ejection Fraction	Ventricular Substrate	Antiarrhythmic Medication
L V15	54, Male	Non-sustained VT	45%	No scar	Lidocaine, $\beta$ -blocker

Table 2

Comparison of noninvasive ECGI with invasive EP study

Patients are identified on the basis of VT localization; RVX for patient X with right ventricular localization; LVX for patient X with left ventricular localization. Discrepancies between ECGI and EPS are highlighted in yellow. LV: left ventricle; RV: right ventricle; RVOT: right ventricular outflow tract; N/A: not available. Because of the thin tissue in the outflow tract, patients with outflow tract SOO were excluded from myocardial depth analysis. Arrhythmias starting from a focal origin and spreading radially in the ECGI activation map are classified as “radial”, as ECGI cannot differentiate between focal mechanism and micro-reentry.

	Localization		Mechanism	Myocardial Depth		
	ECGI	EPS		ECGI	EPS	
<b>RIGHT VENTRICLE</b>						
<b>RV1</b>	Anterior-left RVOT	Anterior-left RVOT	Radial	Focal	Excluded	Excluded
<b>RV2</b>	Mid-septal RVOT	Mid-septal RVOT	Radial	Focal	Excluded	Excluded
<b>RV3</b>	Mid-septal RVOT	Mid-septal RVOT	Radial	Focal	Excluded	Excluded
<b>RV4</b>	Posterior-right RVOT	Posterior-right RVOT	Radial	Focal	Excluded	Excluded
<b>RV5</b>	Anterior-left RVOT	N/A	Radial	N/A	Excluded	Excluded
<b>RV6</b>	Free wall RVOT	Free wall RVOT	Radial	Focal	Excluded	Excluded
<b>RV7</b>	Mid-septal RVOT	Mid-septal RVOT	Radial	Focal	Excluded	Excluded
<b>RV8</b>	Free wall RVOT	Free wall RVOT	Radial	Focal	Excluded	Excluded
<b>RV9</b>	Mid-septal RVOT	Mid-septal RVOT	Radial	Focal	Excluded	Excluded
<b>RV10</b>	Inferior basal lateral RV	Inferior basal septal RV	Radial	Focal	Epicardial	Epicardial
<b>RV11</b>	Posterior-right RVOT	Posterior-right RVOT	Radial	Focal	Excluded	Excluded
<b>LEFT VENTRICLE</b>						
<b>LV1</b>	Lateral apical LV	Lateral apical LV	Radial	Focal	Epicardial	Epicardial
<b>LV2</b>	Inferior basal septal LV	Inferior basal septal LV	Reentry	Reentry	Fractionated	Endocardial
<b>LV3</b>	Inferior lateral apical LV	Inferior lateral apical LV	Reentry	Reentry	Fractionated	Midmyocardial
<b>LV4</b>	Apical septal LV	Fascicular	Radial	Focal	Intramural	Endocardial
<b>LV5</b>	Apical septal LV	Fascicular	Radial	Focal	Intramural	Endocardial
<b>LV6</b>	Anterior basal LV	Anterior basal LV	Radial	Focal	Epicardial	Epicardial
<b>LV7</b>	Left coronary cusp	Left coronary cusp	Radial	Focal	Excluded	Excluded
<b>LV8</b>	Lateral basal LV	N/A	Reentry	N/A	Epicardial	N/A
<b>LV9</b>	Septal basal LV	Septal basal LV	Reentry	Reentry	Fractionated	Endocardial

	Localization		Mechanism		Myocardial Depth	
	ECGI	EPS	ECGI	EPS	ECGI	EPS
<b>LV10</b>	Septal basal LV	N/A	Radial	N/A	Epicardial	N/A
<b>LV11</b>	Anterior LV	Apical LV	Reentry	Reentry	Fractionated	Midmyocardial
<b>LV12</b>	Inferior basal LV	N/A	Reentry	N/A	Fractionated	N/A
<b>LV13</b>	Lateral basal LV	Lateral basal LV	Radial	Focal	Epicardial	Epicardial
<b>LV14</b>	Mid anterior LV	Mid anterior LV	Reentry	Reentry	Fractionated	Endocardial
<b>LV15</b>	LV summit	Great cardiac vein	Radial	Focal	Epicardial	Epicardial